Diffusivity interfaces in lattice Monte Carlo simulations: Modeling inhomogeneous delivery and release systems

M. Ignacio,[1,*] M. Bagheri,[1] M. V. Chubynsky,[1,†] H. W. de Haan,[2] and G. W. Slater[1]
[1]*Department of Physics, University of Ottawa, Ottawa, Ontario K1N 6N5, Canada*
[2]*Department of Physics, Ontario Tech University, Oshawa, Ontario L1H 7K4, Canada*

(Received 4 March 2022; accepted 13 June 2022; published 29 June 2022)

Lattice Monte Carlo (LMC) simulations are widely used to investigate diffusion-controlled problems such as drug-release systems. The presence of an inhomogeneous diffusivity environment raises subtle questions about the interpretation of stochastic dynamics in the overdamped limit, an issue sometimes referred to as the "Ito-Stratonovich-isothermal dilemma." We propose a LMC formalism that includes the different stochastic interpretations in order to model the diffusion of particles in a space-dependent diffusivity landscape. Using as an example a simple inhomogeneous one-dimensional system with a diffusivity interface and different boundary conditions, we demonstrate that we can properly reproduce the steady state and dynamic properties of these systems and that these properties do depend on the choice of calculus. In particular, we argue that the version of the LMC algorithm that uses Ito calculus, which is commonly used to model drug delivery systems, should be replaced by the isothermal version for most applications. Our LMC methodology provides an efficient alternative to Langevin simulations for a wide class of space-dependent diffusion problems.

DOI: 10.1103/PhysRevE.105.064135

I. INTRODUCTION

Lattice Monte Carlo (LMC) algorithms are very popular and efficient methods to model nontrivial diffusion problems. For instance, LMC simulations are frequently used to study drug-release systems with different diffusivity regions, irregular shapes, and/or complex loading patterns [1–5].

The fundamental quantities required to build LMC simulation algorithms are the probabilities (or rates) for each allowed transition, and the latter must take into account the local environment (most naturally, in the form of their dependence on the properties of the medium at the neighboring sites). For a particle diffusing in a homogeneous diffusivity landscape, the expressions for the hopping probabilities and time steps are fairly straightforward, although there is a nontrivial specific choice of these parameters that needs to be made if an optimal algorithm that properly reproduces the fourth moment of the particle distribution is required [6]. However, as soon as the system possesses diffusivity interfaces or gradients, a subtle problem emerges: What should be the hopping probability across the interface? In other words, how should the jumping probabilities take into account the fact that the next site is not identical to the starting site? This issue, the "Ito-Stratonovich-isothermal dilemma," naturally appears from a Langevin formalism in the overdamped limit and can impact both the dynamic and the stationary properties of the system [7,8].

Most of the simulations presented in the drug-delivery literature implicitly, often without discussion, use LMC algorithms based on the Ito interpretation in which the hopping probabilities only depend on the diffusion coefficient at the starting point of the LMC "jump." However, simulation results are generally compared to analytical calculations that are consistent with the isothermal interpretation [9–12]. We also note that in the case of drug-delivery systems, the external environment is often treated as an absorbing boundary, an approximation that does not allow the drug molecules to diffuse back into the system. However, the probability of jumping toward this boundary may in principle depend on the diffusivity in the external environment. Correctly treating the boundary conditions is thus critical to properly modeling a broad class of release systems.

In this article, we propose hopping probabilities (and time durations) for each choice of stochastic calculus, and we examine the impact of that choice on the properties of simple diffusion-controlled systems. The article is structured as follows. We first review some basic elements of the theory of diffusion in one dimension (1D). We then derive the hopping probabilities and time steps for LMC simulations. We test our LMC algorithm on two simple 1D systems and discuss dynamic and stationary properties: First we study a closed system with reflecting boundary conditions (BC), and then a release system modeled with an absorbing BC. In both cases, we have two regions with different diffusivities separated by a sharp interface.

II. PARTICLES WITH A POSITION-DEPENDENT DIFFUSION COEFFICIENT

Let us consider a one-dimensional system of noninteracting identical particles diffusing in a fluid in contact with a thermostat at temperature T and characterized by a space-dependent diffusion coefficient $D(x)$. A standard way to study

*Corresponding author: maxime.ignacio@gmail.com
†Present address: Mathematics Institute, University of Warwick, Coventry CV4 7AL, United kingdom.

such systems consists in writing a Langevin equation for each particle, or tracer, in order to obtain a set of trajectories and then compute ensemble averages over the whole set of trajectories.

We first examine the situation where the diffusivity D is uniform in space. In this case, the corresponding discretized overdamped Langevin equation for the displacement Δx of a particle is straightforward:

$$\Delta x = \sqrt{2D\Delta t}\,\xi_{\Delta t}, \tag{1}$$

where $\sqrt{2D}$ is called the noise multiplicative term and $\xi_{\Delta t}$ is a random number drawn at each time step Δt and obeying a Gaussian distribution with $\langle \xi_{\Delta t}\rangle = 0$, $\langle \xi_{\Delta t}^2\rangle = 1$ and no correlation between different time intervals. The brackets $\langle \cdots \rangle$ represent an ensemble average over all possible realizations of ξ during the time Δt. Physically speaking, $\xi_{\Delta t}$ can be viewed as the result of a multitude of short, small-amplitude "kicks" induced by the collisions with fluid particles [13].

However, if D is a continuous function of x (and is thus an implicit function of t), a subtlety appears since we then need to specify the position x (or equivalently the time t) at which the term $\sqrt{2D(x)}$ has to be estimated in the interval $\Delta x = x(t+\Delta t) - x(t)$. As a consequence, Eq. (1) can be written as [7]

$$\Delta x = \sqrt{2D(x+\alpha\Delta x)\Delta t}\,\xi_{\Delta t}, \tag{2}$$

where the parameter α can in principle take any value in the interval $\alpha \in [0;1]$. In practice, only the values $\alpha = 0$ (Ito calculus: the diffusivity is estimated at the beginning of the jump), $\alpha = 1/2$ (Stratonovich: at the middle of the jump), and $\alpha = 1$ (isothermal: at the end of the jump) have a physical meaning [14,15].

The fact that the noise multiplicative term is ill defined is often called the Ito-Stratonovich-isothermal dilemma. As we will show later, the choice of α (also called the rule of integration) can change both the dynamics and static properties of drug-delivery systems.

Using the series expansion

$$D(x+\alpha\Delta x) \approx D(x) + \alpha\,\tfrac{dD(x)}{dx}\,\Delta x + \mathcal{O}(\Delta x^2), \tag{3}$$

we can rewrite Eq. (2) as (see Appendix A)

$$\Delta x = \alpha\tfrac{dD(x)}{dx}\Delta t + \sqrt{2D(x)\Delta t}\,\xi_{\Delta t}. \tag{4}$$

In this expression, the *noise-induced drift velocity* $\alpha\frac{dD}{dx}$ [16] acts in the direction of the diffusivity gradient (but is zero in the case of Ito calculus, $\alpha = 0$).

Alternatively, rather than using the Langevin formalism, the evolution of the system can be obtained by solving the Fokker-Planck equation for the particle concentration $C(x,t)$. The passage from the Langevin equation to the Fokker-Planck equation is done using the Kramers-Moyal expansion [17]. In this case, the concentration obeys the conservation law

$$\tfrac{\partial}{\partial t}C(x,t) = -\tfrac{\partial}{\partial x}J(x,t), \tag{5}$$

where $J(x,t)$ is the particle flux [7]

$$J(x,t) = \underbrace{-(1-\alpha)\,C\,\tfrac{\partial D}{\partial x}}_{\text{Diffusion drift}}\underbrace{-D\,\tfrac{\partial C}{\partial x}}_{\text{Fick's law}}. \tag{6}$$

The "diffusion drift" term, which is a flux added to the classical Fick term, points in the direction opposite to the diffusivity gradient. This term is zero only for the isothermal case ($\alpha = 1$). Using Eqs. (5) and (6), a general expression for the diffusion equation is obtained:

$$\frac{\partial}{\partial t}C(x,t) = (1-\alpha)\frac{\partial}{\partial x}\left[C\frac{\partial D}{\partial x}\right] + \frac{\partial}{\partial x}\left[D\frac{\partial C}{\partial x}\right]. \tag{7}$$

Assuming that an equilibrium state exists, the flux is $J(x, t\to\infty) = 0$ everywhere (e.g., the equilibrium state of a system confined between two reflecting walls). In this case, the solution to Eq. (6) must be of the form

$$C(x)D(x)^{1-\alpha} = \text{const.} \tag{8}$$

For the isothermal ($\alpha = 1$) case, Eq. (8) predicts a uniform equilibrium (steady-state) concentration $C(x, t\to\infty) = C_\infty$, consistent with the Boltzmann distribution in the absence of external potentials. However, for $\alpha = 0$ or $1/2$, the equilibrium (stationary) concentration depends explicitly on the space-dependent diffusion coefficient $D(x)$.

If the diffusivity $D(x)$ is changing very rapidly (so that it can be considered essentially discontinuous; see Ref. [7] for a discussion about this concept) at points x_i, the concentration $C(x,t)$ can be obtained by solving Eq. (7) for each region where the diffusivity is continuous, and then connecting the piecewise solutions at the interfaces x_i using the continuity conditions

$$C(x_i^-,t)D^{1-\alpha}(x_i^-) = C(x_i^+,t)D^{1-\alpha}(x_i^+) \tag{9}$$

and

$$J(x_i^-,t) = J(x_i^+,t), \tag{10}$$

while also applying the BCs. For example, an analytical "isothermal" solution for a spherical core-shell system using Laplace transforms is given in Refs. [9,18]. However, obtaining an analytical expression for $C(x,t)$ can be difficult (if not impossible), depending on $D(x)$, the initial state $C(x,0)$, and the BCs. Numerical methods, including particle simulations, are often more convenient. In the next section, we derive analytical expressions for the hopping probabilities and jump times required for a LMC algorithm to properly reproduce the behavior predicted by Eq. (7), thus offering a reliable simulation method for complex problems.

III. LMC ALGORITHM WITH FIXED SPATIAL AND TIME STEPS

We employ a LMC scheme where both the time step $\Delta t = \tau$ and the square lattice step $\Delta x = a$ are fixed, and particles can only jump between nearest neighbor lattice sites. To ensure microscopic reversibility at equilibrium, the hopping probabilities P must satisfy the detailed balance between adjacent lattice sites i and $i+1$,

$$C_i P_{i\to i+1} = C_{i+1}P_{i+1\to i}, \tag{11}$$

where C_i is the stationary concentration of particles on site i.

We can then use the stationary condition (8) for two adjacent sites:

$$C_i D_i^{1-\alpha} = C_{i+1}D_{i+1}^{1-\alpha}. \tag{12}$$

Using this relation and Eq. (11), we obtain the local ratio between the hopping probabilities

$$\frac{P_{i+1\to i}}{P_{i\to i+1}} = \left(\frac{D_{i+1}}{D_i}\right)^{1-\alpha}. \tag{13}$$

In order to obtain the probabilities themselves, we need an expression linking local dynamics to local parameters; we propose to use the simple expression

$$P_{i+1\to i} + P_{i\to i+1} = 2D^*\tau/a^2, \tag{14}$$

where $D^* \equiv D^*(i, i+1;\alpha) = D^*(i+1, i;\alpha)$ is an effective local diffusivity with a value between D_i and D_{i+1}. In principle, the choice of D^* is not unique since any symmetric expression would give the correct ratio $P_{i+1\to i}/P_{i\to i+1}$. Moreover, since D^* is multiplied by the arbitrary iteration time step τ, its value does not influence our simulation results here (data not shown). However, for reasons described in Appendix B, we use the expression

$$D^* = \frac{D_i^\alpha D_{i+1}^\alpha \left(D_i^{1-\alpha} + D_{i+1}^{1-\alpha}\right)}{D_i^\alpha + D_{i+1}^\alpha}. \tag{15}$$

Choosing this expression has the advantage of giving the correct first-passage probabilities in a particular case when the interface is equidistant between two lattice sites. Interestingly, the effective diffusivity D^* corresponds to the arithmetic mean of D_i and D_{i+1} for $\alpha = 0$ (Ito), to the geometric mean for $\alpha = 1/2$ (Stratonovitch), and to the harmonic mean for $\alpha = 1$ (isothermal). Note that they are ordered as follows: $D^*(\alpha = 1) \leqslant D^*(\alpha = 1/2) \leqslant D^*(\alpha = 0)$.

Finally, using Eqs. (13)–(15), we obtain

$$P_{i\to i\pm1} = \frac{\tau}{a^2} \times \begin{cases} D_i, & \text{if } \alpha = 0, \\ \frac{2D_i\sqrt{D_{i\pm1}}}{\sqrt{D_i}+\sqrt{D_{i\pm1}}}, & \text{if } \alpha = 1/2, \\ \frac{2D_iD_{i\pm1}}{D_i+D_{i\pm1}}, & \text{if } \alpha = 1. \end{cases} \tag{16}$$

Although the time step τ is arbitrary, its choice must ensure that $P_{i\to i} = 1 - P_{i\to i-1} - P_{i\to i+1} \geqslant 0$ for all sites ($P_{i\to i}$ is the probability to remain at the same lattice site); therefore, τ must satisfy the inequality

$$\tau \leqslant a^2/2D_{\max}, \tag{17}$$

where $D_{\max} \equiv \max\{D_i\}$.

In the uniform case $D(x) = D^* = D_0$, the time step $\tau = a^2/2D_0$ leads to the *classical* LMC scheme for 1D Brownian motion with $P_{i\to i\pm1} = 1/2$ and $P_{i\to i} = 0$. The alternative choice $\tau = a^2/6D_0$ leads to the *optimal* LMC scheme [6] with $P_{i\to i\pm1} = 1/6$ and $P_{i\to i} = 2/3$. Unfortunately, if the diffusion coefficient is space dependent, it is not possible to obtain optimal hopping probabilities for all sites; Eq. (17) is then an appropriate simple choice.

We note that for $\alpha = 1$, Eq. (16) gives $P_{i\to i+1} = P_{i+1\to i}$, which obviously leads to a uniform steady-state concentration, hence the name isothermal calculus. On the other hand, Eq. (16) gives $P_{i\to i\pm1} = D_i\tau/a^2$ when $\alpha = 0$: The hopping probabilities then only depend on the diffusivity at the starting site, the main characteristic of Ito calculus, the most frequent choice in kinetic LMC algorithms [19–21]. As we will see, these two choices can give very different simulation results.

Strictly speaking, the term Monte Carlo refers to the use of random numbers to select (or reject) a new configuration (or state), such as in the Metropolis algorithm [22]. Instead of using particle-based Lattice Monte Carlo simulations as such, we will use a much more efficient method based on *Markov chains*. In essence, this method essentially enumerates all possible trajectories for a finite number of jumps [23–26]. The result is thus the same as if we were using random-number-based particle LMC simulations with an infinite ensemble size (our "simulation" data are thus numerically exact, i.e., without statistical noise, a useful feature for testing purposes).

IV. RESULTS

We now investigate the relaxation-release dynamics of particles for two classes of systems with a piecewise uniform diffusivity landscape. In Sec. IV C, we examine a delivery system located into an empty reservoir surrounded by a wall. However, drug-delivery systems are often modeled using a perfectly adsorbing boundary condition instead of an external reservoir; a generalized version of such a setup is studied in Sec. IV D.

A. Systems with a piecewise uniform diffusivity

We consider a 1D system of length $L = L_- + L_+$ with a piecewise diffusivity $D(x) = D_-$ if $x \in [-L_-; 0[$ (the–side) and $D(x) = D_+$ if $x \in [0; L_+]$ (the + side). The system is discretized into $N = L/a$ lattice sites of size a. The continuity conditions (9) and (10) then read

$$C(0^-, t)\, D_-^{1-\alpha} = C(0^+, t)\, D_+^{1-\alpha} \tag{18}$$

and

$$D_- \left.\frac{\partial C}{\partial x}\right|_{0^-} = D_+ \left.\frac{\partial C}{\partial x}\right|_{0^+}. \tag{19}$$

The initial concentration $C(x, 0)$ is chosen to be uniform on the–side, $C(x < 0, 0) = C_0$, while the + side starts empty, $C(x > 0, 0) = 0$. The time evolution of the system is to be studied as a function of the ratio D_+/D_- by keeping D_- constant and varying D_+. The LMC time step is $\tau = a^2/(2\max[D_-, D_+])$ and the diffusion time $\tau_- = L_-^2/2D_-$ is used to rescale all times.

In Sec. IV C, the system as a whole is between two reflecting boundaries which must satisfy

$$\partial_x C(x, t)|_{x=\pm L_\pm} = 0, \tag{20}$$

while Sec. IV D treats the case of an absorbing boundary at $x = L_+$,

$$C(x, t)|_{x=L_+} = 0. \tag{21}$$

Unless otherwise stated, our focus will be systems with two equal parts of size $L_+ = L_- = L/2$, with $N = 100$. However, we will also discuss the $L_+ \ll L_-$ and $L_+ \gg L_-$ cases since they are both of practical interest.

B. Basic definitions and global relaxation times

Ideally, we want to use physical quantities that describe the evolution of the initial system, i.e., where the particles are initially located, independent of the nature of the boundary

conditions or external world. In particular, we want to follow the time evolution of both the concentration profile $C(x,t)$ and the number of particles left in the system, which is defined given by

$$N_-(t) = \int_{-L_-}^{0} C(x,t)\,dx. \tag{22}$$

In the presence of absorbing boundary conditions, the steady-state concentration is trivially $C(x, t \to \infty) = 0$. However, by dividing the concentration by its average value in the system at time t,

$$\tilde{C}(x,t) = \frac{C(x,t)}{L^{-1}\int_{-L_-}^{L_+} C(x,t)\,dx}, \tag{23}$$

we obtain a dimensionless description of the distribution of the remaining particles.

Similarly, we define the normalized amount of particles present in the release system at time t as

$$\rho_-(t) = \frac{N_-(t) - N_-(\infty)}{N_-(0) - N_-(\infty)}. \tag{24}$$

Note that $\rho_-(t)$ decays from 1 at $t = 0$ to 0 when $t \to \infty$.

For this class of problems (i.e., systems bounded by reflective and/or absorbing boundaries), the normalized quantity $\rho_-(t)$ decays as a sum of exponentials [27],

$$\rho_-(t) = \sum_{n=0}^{+\infty} A_n^* \exp\left(-\frac{t}{\tau_n}\right), \tag{25}$$

where A_n^* and τ_n are the weights and relaxation times of the nth mode, respectively, and both depend on the set of variables $\{D_-, D_+, L_-, L_+, \alpha\}$.

The longest relaxation time in Eq. (25), $\tau_{n=0}$, which can be obtained from the inverse slope (on a semilogarithmic plot) of the long-time exponential decay, is often defined as the overall process relaxation time. However, this can be misleading when the initial conditions are such that the weight A_0^* is small since relaxation is then mostly happening at shorter times (an example of short time dynamics is shown in the inset of Fig. 2). Instead, we use the surface under the curve $\rho_-(t)$ to estimate the global relaxation time [5,28]

$$\tau_-^* = \int_0^\infty \rho_-(t)\,dt = \sum_{n=0}^{\infty} A_n^*\,\tau_n. \tag{26}$$

Note that τ_-^* is effectively a weighted average over all relaxation modes.

For systems in which molecules have a space-dependent diffusivity $D(x)$ and/or a nonuniform initial loading $C(x,0)$, such as core-shell structures [9], it is tedious to obtain analytical expressions for the parameters A_n^* and τ_n. However, it is easier to calculate τ_-^* because we then only need to solve the time integrated equation of diffusion—see Appendix C.

We can derive the general asymptotic behaviors of Eq. (25). For short times, $t \ll \tau_-^*$, we obtain

$$\rho_-(t) \approx 1 - \sqrt{t/\tau_i}, \tag{27}$$

where the *initial diffusion time* τ_i depends on the diffusion conditions at the interface. For long times $t \gg \tau_-^*$, only the longest relaxation time τ_0 remains and we obtain

$$\rho_-(t) \approx A_0^* \exp(-t/\tau_0), \tag{28}$$

where $0 < A_0^* \leqslant 1$. The preferred way [5] to plot $\rho_-(t)$ versus t in order to extract useful information about the physical mechanisms at play is to use the triple-log representation $\ln[-\ln[\rho_-(t)]]$ vs $\ln[t]$ (we will use this approach in the following).

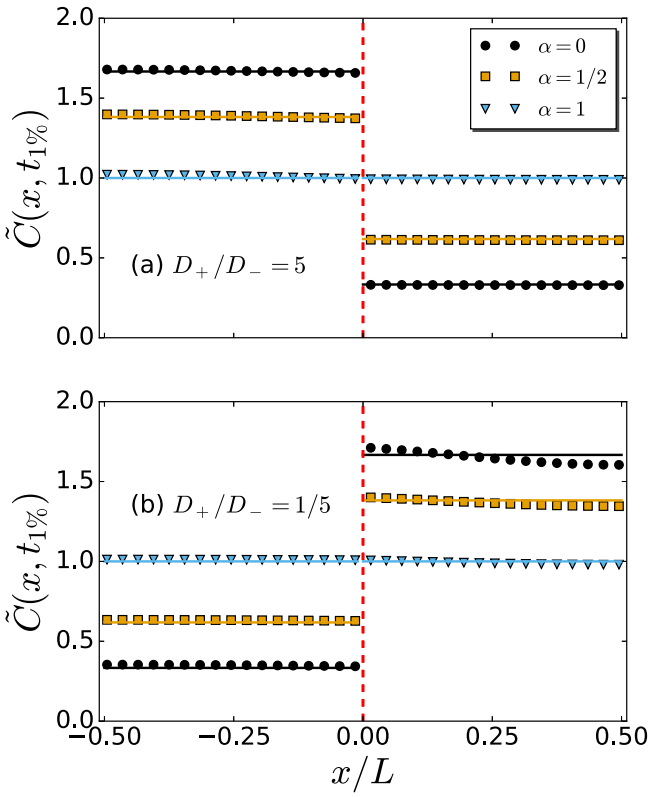

FIG. 1. Two reflecting boundaries: dimensionless concentration $\tilde{C}(x,t)$ vs x/L for (a) $D_+/D_- = 5$; (b) $D_+/D_- = 1/5$. The symbols correspond to LMC data at time $t_{1\%}$ defined by $\rho_-(t_{1\%}) = 1\%$; the solid lines show the analytical predictions given by Eq. (29). The vertical dashed line marks the position of the interface.

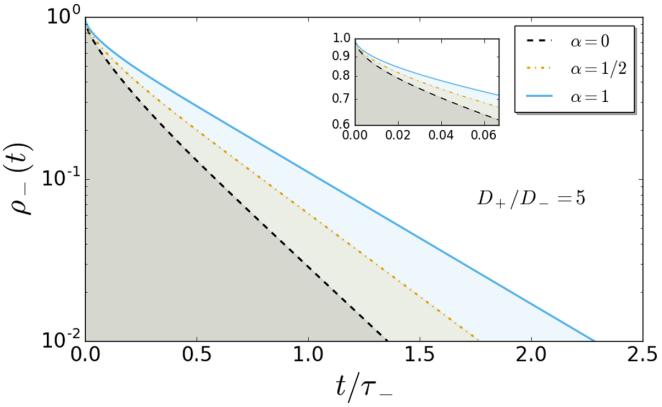

FIG. 2. Two reflecting boundaries: $\rho_-(t)$ vs time for the three calculi and $D_+/D_- = 5$ (LMC data). The inset shows the nonexponential behavior at short times.

C. A system between two reflecting boundaries

We first consider a system with two reflecting boundaries satisfying Eq. (20) (with $L_+ = L_- = L/2$). Basically, the $-$ side is the drug delivery system (such as a hydrogel) while the $+$ side is the reservoir in which it is immersed. The drug leaks out of the delivery system until an equilibrium is reached with the reservoir. In this case, the total number of particles $N_{\rm tot} = \int_{-L/2}^{+L/2} C(x,t)\,dx = C_0 L/2$ is conserved, while Eqs. (8) and (23) predict that the equilibrium normalized concentration is then given by

$$\tilde{C}(t\to\infty) = \frac{2}{D_-^{1-\alpha}+D_+^{1-\alpha}} \times \begin{cases} D_+^{1-\alpha}, & \text{if } x<0. \\ D_-^{1-\alpha}, & \text{if } x>0. \end{cases} \tag{29}$$

Note that $\tilde{C}(t\to\infty) \equiv \tilde{C}_{eq}$ is uniform only if $\alpha = 1$ (the isothermal calculus). For $\alpha = 0$ and $1/2$, the diffusivity gradient leads to a flux from the high diffusivity region to the low diffusivity one, and particles thus accumulate in the latter. Dimensionless concentration profiles $\tilde{C}(x, t_{1\%})$ are shown in Figs. 1(a) for $D_+/D_- = 5$ and 1(b) for $D_+/D_- = 1/5$, where $t_{1\%}$ is the time at which $\rho_-(t) = 1\%$. Our long-time LMC data (symbols) agree with the analytical prediction, Eq. (29). Only isothermal calculus gives a continuous concentration profile across the interface and a uniform concentration in equilibrium. Interestingly, Eq. (18), coupled with the fact that the total amount of particles is conserved when we use two reflective walls, leads to the three curves being in reverse order on both sides of the interface. As we shall see later (see Fig. 5), a similar inversion can also occur in the presence of an absorbing wall.

The time evolution of $\rho_-(t)$ (LMC data) for the three calculi is shown in Fig. 2 for $D_+/D_- = 5$. Although the long-time decay is clearly exponential, the inset shows that higher modes play a role at short time. However, a semilog plot is not ideal here. Instead, Fig. 3 shows the data using a triple-log representation for (a) $D_+/D_- = 5$ and (b) $D_+/D_- = 1/5$. The expected slopes for short [=12, Eq. (27)] and long [=1, Eq. (28)] times are shown in red. The qualitative behavior of $\rho_-(t)$ is identical in both limits: $\rho_-(t;\alpha=0) < \rho_-(t;\alpha=1/2) < \rho_-(t;\alpha=1)$.

For this symmetric system (i.e., $L_+ = L_- = L/2$), the analytical expression for the global relaxation time is

$$\frac{\tau_-^*}{\tau_-} = \frac{2}{3}\frac{D_-}{D^*}, \tag{30}$$

where D^* is given by Eq. (15). This exact result is compared to LMC data in Fig. 4: The data perfectly match the analytical prediction. We thus conclude that our algorithm gives the right final states and relaxation times for all three calculi. Interestingly, we observe that $\tau_-^*(\alpha=1) > \tau_-^*(\alpha=1/2) > \tau_-^*(\alpha=0)$ for all ratios D_+/D_- except when $D_+/D_- = 1$ (uniform diffusivity) where $\tau_-^*/\tau_- = 2/3$ (the choice of the calculus does not matter in a uniform system).

The generalization of Eq. (30) for an asymmetric system of total length $L = L_- + L_+$ reads

$$\frac{\tau_-^*}{\tau_-} = \frac{2}{3}\left[1 - \frac{1-\frac{D_-L_+^2}{D_+L_-^2}}{1+\frac{L_+}{L_-}\left(\frac{D_-}{D_+}\right)^{1-\alpha}}\right]. \tag{31}$$

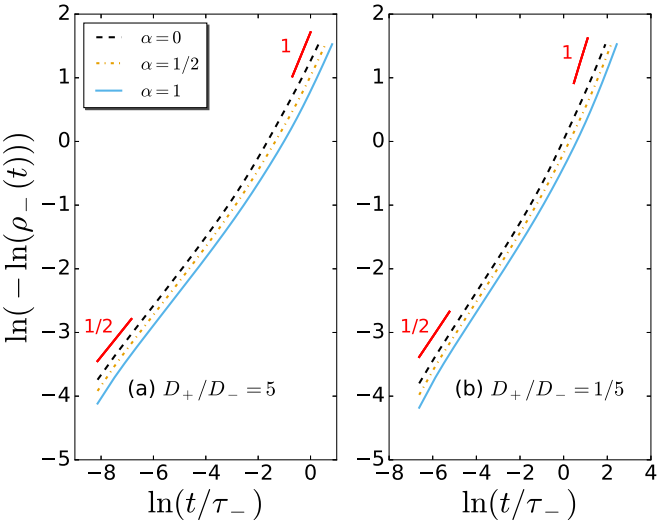

FIG. 3. Two reflecting boundaries: triple-log plot of $\rho_-(t)$ *vs* time for the three calculi (LMC data) (a) $D_+/D_- = 5$; (b) $D_+/D_- = 1/5$. The expected slopes for short ($1/2$) and long (1) times are shown in red.

Equations (30) and (31) can be derived using an approach similar to the one used in Appendix C.

There are two interesting reservoir size limits here. First, when $L_+/L_- \ll 1$, we find that

$$\tau_-^* \approx \frac{1}{3}\frac{L_+L_-}{D_-^{\alpha}D_+^{1-\alpha}}. \tag{32}$$

We note that τ_-^* is then independent of D_- for Ito, independent of D_+ for isothermal and symmetric with respect to D_- and D_+ for Stratonovich calculus. However, it is important to stress that these results do not imply that the full release process is independent of D_- or D_+, respectively, for $\alpha = 0$ or 1; see Appendix D for details.

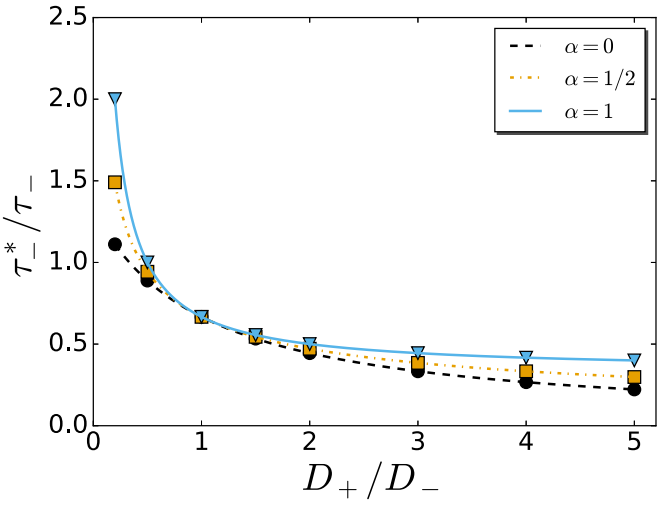

FIG. 4. Two reflecting boundaries: Scaled relaxation time τ_-^*/τ_- vs diffusivity ratio D_+/D_-. The symbols correspond to LMC data and the solid lines to Eq. (30).

Conversely, for $L_+/L_- \gg 1$ (the large reservoir limit), we obtain

$$\tau_-^* \approx \frac{1}{3}\frac{L_+L_-}{D_+^\alpha D_-^{1-\alpha}}. \tag{33}$$

Note that Eqs. (33) and (32) just differ by a permutation of the signs + and–,which naturally implies that τ_-^* is the same in both limits for $\alpha = 1/2$.

D. Using an absorbing boundary

We now replace the reflecting BC at $x = L_+$ by an absorbing one (i.e., a perfect sink), following Eq. (21). There are three ways to interpret this type of system. If $L_+ = 0$, this is equivalent to the standard approach of modeling a release system by imposing an absorbing boundary condition at its surface. If $L_+ > 0$, the + region can be seen as the shell of a two-phase delivery system, again with an absorbing boundary at its surface (in most cases, we would then have $0 < L_+ \leqslant L_-$ and $D_+ < D_-$). This type of system has been extensively studied using Ito-calculus LMC in the field of drug release, especially in the $L_+ = 0$ limit [4,9,11,12,29–32], but it is also possible to see the $L_+ > 0$ case as the release of drugs into a large outside volume which is surrounded by an absorbing boundary at a distance L_+.

In this case, the analytical expressions for the equilibrium concentration are

$$\tilde{C}(x) = \begin{cases} \tilde{C}_- \cos \frac{x+L_-}{(D_-\tau_0)^{1/2}}, & \text{if } x < 0, \\ \tilde{C}_+ \sin \frac{L_+-x}{(D_+\tau_0)^{1/2}}, & \text{if } x > 0, \end{cases} \tag{34}$$

where $\tilde{C}_-$, $\tilde{C}_+$, and τ_0 have to calculated numerically (except for $\alpha = 1/2$ where analytical expressions can be found); see Appendix E for details.

As before, our numerical example will use $L_+ = L_- = L/2$. Dimensionless concentration profiles $\tilde{C}(x, t_{1\%})$ are shown in Fig. 5, together with the analytical forms presented in Eq. (34), for (a) $D_+/D_- = 5$ and (b) $D_+/D_- = 1/5$. Once more, only isothermal calculus gives continuous concentration profiles. We observe a near-linear concentration gradient (hence a flux) between the end of the drug-delivery system ($x = 0$), which acts as a source, and the absorbing boundary (the sink, at $x/L = 1/2$). Although the three curves appear to cross at a universal point near $x/L \simeq -0.3$, high-precision calculations show that this is not the case (i.e., there are three different crossover points; result not shown).

Figure 6 shows the evolution of $\rho_-(t)$ using the triple-log representation. There is a striking difference between the three calculi here: The order $\rho_-(t;\alpha = 0) > \rho_-(t;\alpha = 1/2) > \rho_-(t;\alpha = 1)$ obtained when $D_+/D_- = 5$ is inverted to $\rho_-(t;\alpha = 0) < \rho_-(t;\alpha = 1/2) < \rho_-(t;\alpha = 1)$ when $D_+/D_- = 1/5$. Nevertheless, the two asymptotic slopes are recovered.

Finally, the global relaxation time is given by

$$\frac{\tau_-^*}{\tau_-} = \frac{2}{3}\left[1 + 3\left(\frac{D_-}{D_+}\right)^\alpha\right]; \tag{35}$$

see Appendix C for the details. Figure 7 shows that the LMC data match the analytical prediction. Interestingly, $\tau_-^*(\alpha = 1) > \tau_-^*(\alpha = 1/2) > \tau_-^*(\alpha = 0)$ when the diffusivity ratio $D_+/D_- < 1$ while $\tau_-^*(\alpha = 1) < \tau_-^*(\alpha = 1/2) < \tau_-^*(\alpha = 0)$ when $D_+/D_- > 1$. Note that Ito calculus predicts a constant value $\tau_-^*/\tau_- = 8/3$, which also corresponds to the case for a homogeneous diffusivity $D_+ = D_-$; in other words, the

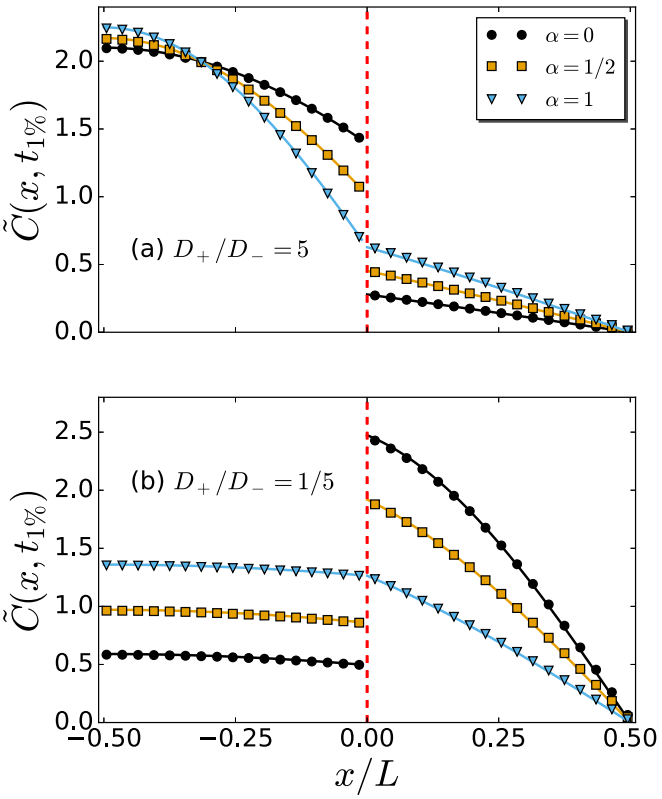

FIG. 5. One absorbing boundary: dimensionless concentration $\tilde{C}(x, t_{1\%})$ vs x/L for (a) $D_+/D_- = 5$; (b) $D_+/D_- = 1/5$. The symbols correspond to LMC data at time $t_{1\%}$ defined by $\rho_-(t_{1\%}) = 1\%$; the solid lines show the analytical predictions given by Eq. (34). The vertical dashed line marks the position of the interface.

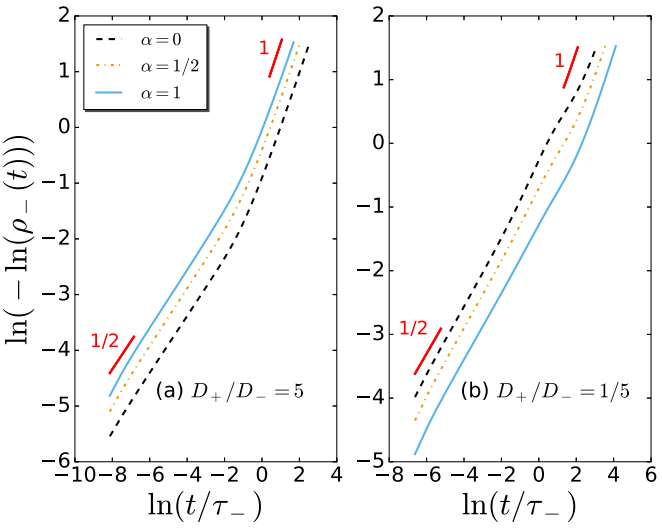

FIG. 6. One absorbing boundary: triple-log plot of $\rho_-(t)$ vs time for the three calculi (LMC data) (a) $D_+/D_- = 5$; (b) $D_+/D_- = 1/5$. The expected slopes for short ($\frac{1}{2}$) and long (1) times are shown in red.

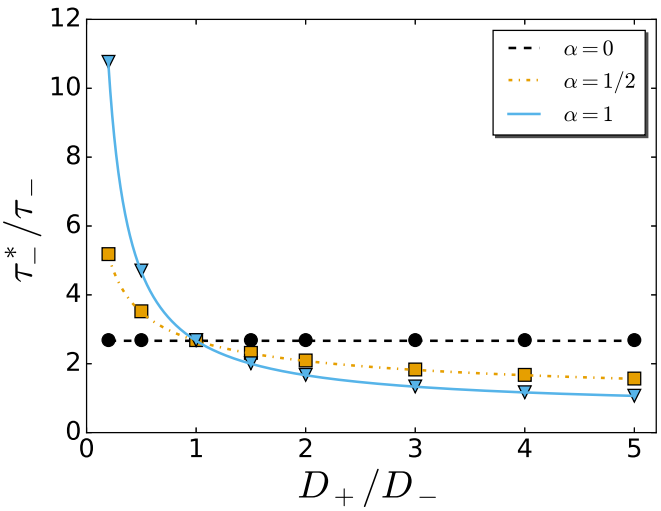

FIG. 7. One absorbing boundary: Scaled relaxation time τ_-^*/τ_- vs diffusivity ratio D_+/D_-. The symbols correspond to LMC data and the solid lines to Eq. (35).

diffusivity in the + region does not impact τ_-^* in the case of Ito calculus, which seems to be an unphysical result.

For an asymmetric system ($L_- \neq L_+$) Eq. (35) becomes

$$\frac{\tau_-^*}{\tau_-} = \frac{2}{3}\left[1 + 3\,\frac{L_+}{L_-}\left(\frac{D_-}{D_+}\right)^{\alpha}\right]. \tag{36}$$

When $L_+/L_- \ll 1$, we basically have a uniform delivery system with a diffusivity D_- and an absorbing boundary at its surface—a standard model used by many authors in the field. We then obtain $\tau_-^*/\tau_- \to 2/3$: Note that the global relaxation time τ_-^* is then independent of the diffusivity in the + zone or the calculus chosen for the simulations. However, this is only true if the "shell" region is of zero width; for finite values of L_+, the release rate, as measured by τ_-^*, does depend on the calculus chosen. In other words, while using Ito calculus might be valid for a uniform system with a thin absorbing boundary at its surface, it cannot be used for core-shell systems (unless there is a physical reason to do so).

Finally, if $L_+/L_- \gg 1$, corresponding to a very large external reservoir, one finds

$$\tau_-^* \approx \frac{L_+ L_-}{D_+^{\alpha} D_-^{1-\alpha}}. \tag{37}$$

which is simply three times larger than the result for two reflecting boundaries, Eq. (33). In this limit, the nature of the boundary condition is of minimal importance.

V. DISCUSSION AND CONCLUSION

Many passive, diffusion-controlled drug delivery systems are composed of different layers through which the drug molecules must diffuse in order to escape and be transferred to an external biological system. Analytical and computational models often replace these layers by structureless zones in which the drug molecules have different diffusion coefficients. In other words, the reduced drug diffusivity due to a layer's finite porosity is replaced by an effective local diffusion coefficient, while the material itself is removed from the problem. Moreover, the external system is generally replaced by an absorbing boundary located at the interface between the delivery system and the external medium. Since these "tricks" greatly simplify modeling and analysis, they have become standard approaches and have indeed led to numerous advances. However, replacing porous materials by effective diffusion coefficients introduces conceptual issues that have been largely neglected although they are critical for lattice Monte Carlo simulations.

In this paper, we have investigated two of these issues: the LMC proper jumping probabilities across a diffusivity interface, and the properties of an absorbing boundary. The additional issue of the lack of free volume conservation (e.g., when a hydrogel region is replaced by a free zone with a reduced diffusivity, the volume available to the drug molecules effectively changes) will be the subject of another paper.

Most particle-based Monte Carlo simulations in the relevant literature implicitly use Ito formalism: The jumping probability depends solely on the diffusivity of the drug molecule on the initial site. We have shown that this generally leads to unphysical results, both in equilibrium (inhomogeneous or discontinuous concentrations—see Fig. 1) and in a drug-delivery scenario (Fig. 5). In order to obtain valid simulation results, one must use isothermal calculus (it is indeed implicitly used in analytical calculations). We have thus introduced a generalized lattice Monte Carlo (LMC) algorithm with fixed time and lattice steps for systems where molecular diffusivity is space dependent. In fact, this LMC scheme can handle diffusion gradients for all three calculi of interest (Ito, isothermal, Stratonovich).

We first tested our LMC algorithm on a simple one-dimensional system with a sharp diffusivity interface and reflecting boundary conditions (i.e., a closed system). Our data show excellent quantitative agreement with theoretical predictions. In particular, they clearly demonstrate that in order to obtain a uniform concentration in equilibrium, one must abandon traditional Ito calculus and use isothermal Monte Carlo instead. We also showed that the relaxation time of the system agrees with the theoretical predictions.

We then studied diffusion-controlled drug-release systems using all three calculi. Again, standard Ito and Stratonovitch LMC data were observed to be generally inconsistent. However, we also showed that the probability of moving across the interface separating a drug delivery system from the outside does not depend on the diffusivity of the molecule on *both* sides on the interface if this interface is treated as a perfect absorber; this is thus the only case where the three calculi give the same result. In the presence of a core-shell structure or an external reservoir, the choice of calculus can have dramatic effects on the release dynamics (see Figs. 3 and 6) and consequently on the system's global relaxation time (see Figs. 4 and 7).

The LMC formalism presented here can easily be used in two and three dimensions (it is also possible to add an external field to the formalism) and with (onion-shaped) systems made of multiple layers. Crucially, the standard Ito Monte Carlo methodology should be replaced by the isothermal one, as described above.

Particle-based simulations with particle-particle collisions (finite drug concentrations) and immobile obstacles (e.g., hard porous walls) can use the algorithm developed here. Our tests

show that it is reliable both in terms of kinetics and equilibrium states.

ACKNOWLEDGMENTS

G.W.S. acknowledges the support of both the University of Ottawa and the Natural Sciences and Engineering Research Council of Canada (NSERC), Funding Reference No. RGPIN/046434-2013.

APPENDIX A: THE NOISE-INDUCED DRIFT TERM

When the diffusivity depends on position (or time), the integration of the stochastic term in the Langevin equation requires one to choose a rule of integration [14]. An alternative method consists in using the series expansion of $D(x+\alpha\Delta x)$ given in Eq. (3); assuming that $|\alpha\frac{dD}{dx}\frac{\Delta x}{D(x)}| \ll 1$, the stochastic term in the overdamped Langevin equation (2) can be written as

$$\sqrt{2D(x+\alpha\Delta x)\Delta t} \approx \sqrt{2D(x)\Delta t}\left(1+\frac{\alpha}{2}\frac{dD}{dx}\frac{\Delta x}{D(x)}\right), \tag{A1}$$

which leads to, keeping terms up to Δt,

$$\begin{aligned}\Delta x &\approx \sqrt{2D\Delta t}\,\xi_{\Delta t}\frac{1}{1-\sqrt{\frac{\Delta t}{2D}}\alpha D'\xi_{\Delta t}},\\ &\approx \sqrt{2D\Delta t}\,\xi_{\Delta t}+\alpha\frac{dD}{dx}\Delta t\,\xi_{\Delta t}^2+\mathcal{O}(\Delta t^{3/2}).\end{aligned} \tag{A2}$$

We want to reproduce the first and second moments of Δx to order Δt; $\langle\Delta x\rangle \approx \alpha\frac{dD}{dx}\Delta t$ and $\langle\Delta x^2\rangle \approx 2D\Delta t$ (only the first two moments will matter over long times because of the central limit theorem). It turns out that one can replace $\xi_{\Delta t}^2$ by $\langle\xi_{\Delta t}^2\rangle = 1$, without any impact on the expressions of $\langle\Delta x\rangle$ and $\langle\Delta x^2\rangle$ given above, which finally leads to Eq. (4).

Physically speaking, Eq. (4) means that the stochastic term is calculated using the position of the particle before the jump, which is the Ito rule of integration ($\alpha = 0$). The other calculi (or stochastic interpretations) are generated by adding the additional deterministic term $\alpha\frac{dD}{dx}$ called the noise-induced drift term.

It is worth noting that this interpretation problem' only appears for overdamped dynamics. Indeed, when the acceleration term ($m\ddot{x}$ in one dimension) is kept, the displacement during one time step is $\sim\Delta t$ instead of $\sim\sqrt{\Delta t}$, the velocity drift is also $\sim\Delta t$, while the difference in velocity between different calculi is $\mathcal{O}(\Delta t^{3/2})$, which is negligible. This is in contrast to the overdamped case, where the difference in Δx between the calculi is $\sim\Delta t$, i.e., the same order as Δx itself.

APPENDIX B: THE EFFECTIVE LOCAL DIFFUSIVITY D^*

The goal of this Appendix is to derive the expression for the local diffusivity D^* given by Eq. (15).

We recall that D^* appearing in the closure relationship [Eq. (14)] can be chosen arbitrarily as long as $D^* = D$ when $D_i = D_{i+1} = D$. We also impose the condition that the effective diffusivity D^* must reproduce correctly the first passage probabilities from sites i and $i+1$ to their neighbours when there is an interface halfway between these sites. This ensures that sequences of visited sites are sampled correctly even for a finite lattice step size a. Note that the choice of the interface position makes sense since dividing the domain into bins with lattice sites in the middle of the bins ensures that the diffusivity is constant within each bin.

For the sake of simplicity, let us assign number 1 to the site immediately to the left of the interface that is located midway between sites 1 and 2. We denote $\mathcal{P}$ the probability that a particle starting at site 1 and governed by the continuum Langevin equation reaches site 2 before site 0. Then to reproduce this probability correctly in our LMC algorithm, we should have

$$\mathcal{P} = \frac{P_{1\to2}}{P_{1\to0}+P_{1\to2}}, \tag{B1}$$

where

$$P_{1\to0} = \frac{D_-\tau}{a^2} \tag{B2}$$

and

$$P_{1\to2} = \frac{2D^*\tau}{a^2}\frac{1}{1+(D_+/D_-)^{1-\alpha}}. \tag{B3}$$

Combining Eqs. (B1), (B2), and (B3), one obtains

$$D^* = \frac{\mathcal{P}D_-}{2(1-\mathcal{P})}\left[1+\left(\frac{D_+}{D_-}\right)^{1-\alpha}\right]. \tag{B4}$$

We now consider an auxiliary lattice with step size $a/2$, with additional sites midway between those of the original lattice, including one at the interface (that we denote 1.5). Consider a particle obeying the Langevin equation. Equivalently, its motion can be represented as a *continuous time* lattice random walk, where the particle moves between adjacent sites when the continuous trajectory, starting at the first site, reaches the second one without visiting any other site. This lattice random walk is unbiased, except possibly at the interface site; this means that the probabilities of moving left and right are always the same (=1/2), except at the interface site where they may be different (we denote them p_- and p_+ for the moves left and right, respectively). It should be kept in mind that the mean time between steps is different on the two sides of the interface (longer by factor D_-/D_+ on the right). This means that to ensure the correct particle concentration, as given by Eq. (8), the frequency of visits to a site (per unit length of the sequence of visited sites) should be proportional to D^α (which will give the probability of being at the site at any given time proportional to $D^{\alpha-1}$, as required). This means that

$$\frac{p_+}{p_-} = \left(\frac{D_+}{D_-}\right)^\alpha \tag{B5}$$

and then, since $p_- + p_+ = 1$,

$$p_- = \frac{D_-^\alpha}{D_-+D_+}, \tag{B6}$$

$$p_+ = \frac{D_+^\alpha}{D_-+D_+}. \tag{B7}$$

We are now in a position to calculate the probability $\mathcal{P}$ that a particle starting at site 1 reaches site 2 before site 0. This can happen in three different ways. First, the particle can move to site 1.5 (probability 1/2) and then from there to

site 2 (probability p_+); the probability of this sequence of two steps is $(1/2)\times p_+$. Second, the particle can move to site 1.5 (probability 1/2), then return to 1 (probability p_-), and from there the probability to get to 2 before 0 is again $\mathcal{P}$; thus, the resulting probability is $(1/2)\times p_-\times\mathcal{P}$. Finally, the particle can move to site 0.5 (to the left of 1; probability 1/2), return to 1 (probability 1/2), and from there the probability is again $\mathcal{P}$; thus, we get for this class of trajectories $(1/2)\times(1/2)\times\mathcal{P}$. Then the resulting equation is

$$\mathcal{P}=\frac{p_+}{2}+\frac{p_-\mathcal{P}}{2}+\frac{\mathcal{P}}{4}, \tag{B8}$$

and the solution is

$$\mathcal{P}=\frac{2p_+}{3p_++p_-}. \tag{B9}$$

Finally, using Eqs. (B6), (B7), and (B4), one gets

$$D^*=\frac{D_-^\alpha D_+^\alpha(D_-^{1-\alpha}+D_+^{1-\alpha})}{D_-^\alpha+D_+^\alpha}. \tag{B10}$$

Note that, of course, we could have considered sites 1, 2 and 3 instead, comparing probabilities to reach sites 1 and 3 from site 2; by symmetry, the result would have been the same. It should also be noted that this derivation is done for the case where the interface is midway between two sites and there is, of course, no reason to assume that it will be valid more generally, say, for the interface at another position or a general continuous change of the diffusivity.

APPENDIX C: DERIVATION OF EQ. (36)

We define $S_\pm(x)=\int_{t=0}^\infty C_\pm(x,t)\,dt$ and integrate the diffusion equation over time to obtain

$$-C_0=D_-\frac{\partial^2 S_-(x)}{\partial x^2}, \tag{C1}$$

for the–region and

$$0=D_+\frac{\partial^2 S_+(x)}{\partial x^2} \tag{C2}$$

for the + region. The boundary conditions for $S(x)$ are similar to those for $C(x,t)$:

$$\left.\frac{\partial S_-}{\partial x}\right|_{x=-L_-}=0 \ \text{ reflecting BC}, \tag{C3}$$

$$S_+(x=L_+)=0 \ \text{ absorbing BC}. \tag{C4}$$

The continuity conditions at the $x=0$ interface are

$$D_-\left.\frac{\partial S_-}{\partial x}\right|_{x=0^-}=D_+\left.\frac{\partial S_+}{\partial x}\right|_{x=0^+}, \tag{C5}$$

$$D_-^{1-\alpha}S_-(0^-)=D_+^{1-\alpha}S_+(0^+). \tag{C6}$$

The solutions for each region are simply

$$\frac{S_-(x)}{C_0\tau_-}=-\left(\frac{x}{L_-}\right)^2-2\left(\frac{x}{L_-}\right)+2\,\frac{L_+}{L_-}\left(\frac{D_-}{D_+}\right)^\alpha, \tag{C7}$$

$$\frac{S_+(x)}{C_0\tau_-}=2\,\frac{D_-L_+}{D_+L_-}\left(1-\frac{x}{L_+}\right). \tag{C8}$$

Finally, we integrate $S_-(x)$ over $x\in[-L_-,0]$ and divide the result by the initial loading $N_0=C_0L_-$: The global relaxation time of the − region is then given by

$$\frac{\tau_-^*}{\tau_-}=\frac{2}{3}\left[1+3\,\frac{L_+}{L_-}\left(\frac{D_-}{D_+}\right)^\alpha\right]. \tag{C9}$$

This reduces to Eq. (35) when $L_\pm=L/2$.

APPENDIX D: THE RELAXATION TIME FOR REFLECTING BOUNDARIES IN THE SMALL AND LARGE LENGTH RATIO LIMITS

For sake of simplicity, let us suppose we start with $C=1$ on the (−) side and $C=0$ on the (+) side.

1. The $L_+/L_-\ll 1$ limit

In this case, except for a very short initial time period ($\sim L_+^2/D_+$), in the lowest-order approximation the concentration on the + side will be equal to the equilibrium one [$\approx(D_-/D_+)^{1-\alpha}$]. Thus, the amount that has escaped in the same approximation is $\approx(D_-/D_+)^{1-\alpha}L_+$. This is time independent; to study the time dependence, we need the next-order approximation. For this, consider the − side, where there will be a depletion region near the interface of size $\sim(D_-t)^{1/2}$. Because of particle number conservation, the characteristic change in the concentration in that region, ΔC, is such that

$$\Delta C(D_-t)^{1/2}\sim(D_-/D_+)^{1-\alpha}L_+. \tag{D1}$$

In this approximation, the concentration on the + side can be determined from the jump condition at the interface and the resulting amount on the + side is

$$(1-k\Delta C)(D_-/D_+)^{1-\alpha}L_+, \tag{D2}$$

where $k\sim 1$, and then

$$\rho_-(t)\sim\Delta C\sim L_+(D_-/D_+)^{1-\alpha}(D_-t)^{-1/2}. \tag{D3}$$

This is invalid at very long times $t\gtrsim L_-^2/D_-$ (when the depletion region would be larger than L_-, which is impossible); at such times ρ_- is exponentially small and can be replaced with zero. It is also invalid at very short times, but as the integral of Eq. (D3) converges at $t\to 0$, this has a negligible effect. Then

$$\tau_-^*\sim\int_0^{L_-^2/D_-}L_+(D_-/D_+)^{1-\alpha}(D_-t)^{-1/2}dt \sim\frac{L_+L_-}{D_-^\alpha D_+^{1-\alpha}}. \tag{D4}$$

2. The $L_+/L_-\gg 1$ limit

Except for a very short initial time period, the concentration is x independent on the − side and equal to $\rho_-(t)$. At not too small times, $\rho_-(t)\ll 1$ (nearly all stuff has escaped). On the + side, near the interface the concentration is $\rho_-(t)(D_-/D_+)^{1-\alpha}$; the size of the region where the concentration is significant is $\sim(D_+t)^{1/2}$. Then from particle number conservation,

$$\rho_-(t)(D_-/D_+)^{1-\alpha}(D_+t)^{1/2}\sim L_-, \tag{D5}$$

and thus

$$\rho_-(t) \sim L_-(D_+/D_-)^{1-\alpha}(D_+t)^{-1/2}. \tag{D6}$$

This is invalid at times $t \gtrsim L_+^2/D_+$, where the whole + side is filled with particles (at this point particle escape stops and ρ_- can be replaced with 0); it is also invalid at short times, which is again negligible. We then obtain

$$\tau_-^* \sim \int_0^{L_+^2/D_+} L_-(D_+/D_-)^{1-\alpha}(D_+t)^{-1/2}dt \sim \frac{L_+L_-}{D_+^\alpha D_-^{1-\alpha}}. \tag{D7}$$

APPENDIX E: THE LONG-TIME DISTRIBUTION $\tilde{C}(x)$ FOR THE CASE WITH ONE ABSORBING BOUNDARY

At long times, only the slowest relaxation mode survives. Let the timescale associated with this mode be τ_0 [so the corresponding decay is $\exp(-t/\tau_0)$]. Then, given the boundary conditions, the spatial dependence is

$$\tilde{C}(x) = \begin{cases} \tilde{C}_- \cos\left[\frac{x+L_-}{(D_-\tau_0)^{1/2}}\right], & \text{if } x < 0. \\ \tilde{C}_+ \sin\left[\frac{L_+-x}{(D_+\tau_0)^{1/2}}\right], & \text{if } x > 0. \end{cases} \tag{E1}$$

The three unknowns here are $\tilde{C}_-$, $\tilde{C}_+$, and τ_0, while the three relevant conditions are as follows:

(1) the jump at the interface

$$D_-^{1-\alpha}\tilde{C}_- \cos\left[\tfrac{L_-}{(D_-\tau_0)^{1/2}}\right] = D_+^{1-\alpha}\tilde{C}_+ \sin\left[\tfrac{L_+}{(D_+\tau_0)^{1/2}}\right], \tag{E2}$$

(2) the flux continuity at the interface

$$\frac{\tilde{C}_-D_-^{1/2}}{\tau_0^{1/2}} \sin\left[\tfrac{L_-}{(D_-\tau_0)^{1/2}}\right] = \frac{\tilde{C}_+D_+^{1/2}}{\tau_0^{1/2}} \cos\left[\tfrac{L_+}{(D_+\tau_0)^{1/2}}\right], \tag{E3}$$

(3) the normalization condition

$$\int_{-L_-}^{L_+} \tilde{C}(x)dx = L = \tilde{C}_+(D_+\tau_0)^{1/2}\left(1 - \cos\left[\tfrac{L_+}{(D_+\tau_0)^{1/2}}\right]\right) + \tilde{C}_-(D_-\tau_0)^{1/2} \sin\left[\tfrac{L_-}{(D_-\tau_0)^{1/2}}\right]. \tag{E4}$$

We can eliminate the ratio $\tilde{C}_-/\tilde{C}_+$ using the first two conditions to obtain an equation for τ_0 as a function of the four system-dependent parameters $D_\pm$ and $L_\pm$:

$$\tan\left[\frac{L_-}{(D_-\tau_0)^{1/2}}\right] \tan\left[\frac{L_+}{(D_+\tau_0)^{1/2}}\right] = \left(\frac{D_+}{D_-}\right)^{\alpha-1/2}. \tag{E5}$$

Equation (E5) needs to be solved numerically (however, note that the special case $\alpha = 1/2$ leads to analytical solutions). Once τ_0 is obtained, Eqs. (E3) and (E4) can be used to obtain properly normalized concentrations $\tilde{C}_\pm(x)$.

[1] P. Lecca, How Monte Carlo heuristics aid to identify the physical processes of drug release kinetics, MethodsX **5**, 204 (2018).

[2] L. Martínez, R. Villalobos, M. Sánchez, J. Cruz, A. Ganem, and L. M. Melgoza, Monte Carlo simulations for the study of drug release from cylindrical matrix systems with an inert nucleus, Int. J. Pharm. **369**, 38 (2009).

[3] R. Villalobos, A. M. Vidales, S. Cordero, D. Quintanar, and A. Domínguez, Monte Carlo simulation of diffusion-limited drug release from finite fractal matrices, J. Sol-Gel Sci. Technol. **37**, 195 (2006).

[4] K. Kosmidis, P. Argyrakis, and P. Macheras, A reappraisal of drug release laws using Monte Carlo simulations: The prevalence of the Weibull function, Pharm. Res. **20**, 988 (2003).

[5] M. Ignacio, M. V. Chubynsky, and G. W. Slater, Interpreting the Weibull fitting parameters for diffusion-controlled release data, Phys. A (Amsterdam, Neth.) **486**, 486 (2017).

[6] M. V. Chubynsky and G. W. Slater, Optimizing the accuracy of lattice Monte Carlo algorithms for simulating diffusion, Phys. Rev. E **85**, 016709 (2012).

[7] H. W. de Haan, M. V. Chubynsky, and G. W. Slater, Monte Carlo approaches for simulating a particle at a diffusivity interface and the "Ito–Stratonovich dilemma", arXiv:1208.5081.

[8] G. Pesce, A. McDaniel, S. Hottovy, J. Wehr, and G. Volpe, Stratonovich-to-Itô transition in noisy systems with multiplicative feedback, Nat. Commun. **4**, 2733 (2013).

[9] A. Hadjitheodorou and G. Kalosakas, Analytical and numerical study of diffusion-controlled drug release from composite spherical matrices, Mater. Sci. Eng. C **42**, 681 (2014).

[10] J. Siepmann and F. Siepmann, Mathematical modeling of drug delivery, Int. J. Pharm. **364**, 328 (2008).

[11] K. Kosmidis and P. Macheras, Monte Carlo simulations of drug release from matrices with periodic layers of high and low diffusivity, Int. J. Pharm. **354**, 111 (2008).

[12] K. Kosmidis and P. Macheras, Monte Carlo simulations for the study of drug release from matrices with high and low diffusivity areas, Int. J. Pharm. **343**, 166 (2007).

[13] N. Van Kampen, *Stochastic Processes in Physics and Chemistry*, 3rd ed. (Elsevier, Amsterdam, 2007).

[14] N. G. van Kampen, Itô versus Stratonovich, J. Stat. Phys. **24**, 175 (1981).

[15] I. Sokolov, Ito, Stratonovich, Hänggi, and all the rest: The thermodynamics of interpretation, Chem. Phys. **375**, 359 (2010).

[16] S. Hottovy, G. Volpe, and J. Wehr, Noise-induced drift in stochastic differential equations with arbitrary friction and diffusion in the Smoluchowski-Kramers limit, J. Stat. Phys. **146**, 762 (2012).

[17] H. Risken, *Fokker-Planck Equation* (Springer, Berlin, 1984).

[18] H. Carlslaw and J. Jaeger, *Conduction of Heat in Solids* (Oxford University Press, London, 1959).

[19] A. B. Bortz, M. H. Kalos, and J. L. Lebowitz, A new algorithm for Monte Carlo simulation of Ising spin systems, J. Comput. Phys. **17**, 10 (1975).

[20] K. A. Fichthorn and W. H. Weinberg, Theoretical foundations of dynamical Monte Carlo simulations, J. Chem. Phys. **95**, 1090 (1991).

[21] M. Kotrla, Numerical simulations in the theory of crystal growth, Comput. Phys. Commun. **97**, 82 (1996).

[22] N. Metropolis, A. W. Rosenbluth, M. N. Rosenbluth, A. H. Teller, and E. Teller, Equation of state calculations by fast computing machines, J. Chem. Phys. **21**, 1087 (1953).

[23] S. Casault and G. W. Slater, Systematic characterization of drug release profiles from finite-sized hydrogels, Phys. A (Amsterdam, Neth.) **387**, 5387 (2008).

[24] S. Casault, M. Kenward, and G. W. Slater, Combinatorial design of passive drug delivery platforms, Int. J. Pharm. **339**, 91 (2007).

[25] I. Majid, D. Ben-Avraham, S. Havlin, and H. E. Stanley, Exact-enumeration approach to random walks on percolation clusters in two dimensions, Phys. Rev. B **30**, 1626 (1984).

[26] A. J. Ellery, R. E. Baker, and M. J. Simpson, Communication: Distinguishing between short-time non-Fickian diffusion and long-time Fickian diffusion for a random walk on a crowded lattice, J. Chem. Phys. **144**, 171104 (2016).

[27] J. Crank, *The Mathematics of Diffusion* (Oxford University Press, London, 1979).

[28] M. Ignacio and G. Slater, Using fitting functions to estimate the diffusion coefficient of drug molecules in diffusion-controlled release systems, Phys. A (Amsterdam, Neth.) **567**, 125681 (2021).

[29] V. Papadopoulou, K. Kosmidis, M. Vlachou, and P. Macheras, On the use of the Weibull function for the discernment of drug release mechanisms, Int. J. Pharm. **309**, 44 (2006).

[30] A. Dokoumetzidis, K. Kosmidis, and P. Macheras, Monte Carlo simulations and fractional kinetics considerations for the Higuchi equation, Int. J. Pharm. **418**, 100 (2011).

[31] M. S. Gomes Filho, F. A. Oliveira, and M. A. A. Barbosa, A statistical mechanical model for drug release: Investigations on size and porosity dependence, Phys. A (Amsterdam, Neth.) **460**, 29 (2016).

[32] D. Caccavo, An overview on the mathematical modeling of hydrogels' behavior for drug delivery systems, Int. J. Pharm. **560**, 175 (2019).